Fabrication of flexible polyindole/carbon nanotube/bacterial cellulose nanofiber nonwoven electrode doped by D-tartaric acid with high electrochemical performance

Wu Jiajia · Du Zhanwen · Xiong Ping · Cai Zhijiang

Abstract The flexible polyindole/carbon nanotube/bacterial cellulose (PIn/CNT/BC) nanofiber nonwoven electrode is prepared by a two-step method combination of 'electrospinning and electrospray' process and potentiostatic polymerization. The structure and morphology of the as-prepared PIn/CNT/BC nonwoven electrode are investigated by Scanning electron microscopy, Transmission electron microscopy, Fourier transform infrared, Brunauer–Emmett–Teller and Energy dispersive spectroscopy. The PIn/CNT/BC electrode has a hierarchy configuration with a broccoli-like rough surface consisting of BC electrospun nanofibers, CNT coating layer and PIn nanoparticle layer, which play the function of supporting substrate, conductive path and electrode active material, respectively. To evaluate the electrochemical properties of PIn/CNT/BC electrode, cyclic voltammetry, galvanostatic charge/discharge and electrochemical impedance spectroscopy tests are performed. The unique structure ensures that the flexible PIn/CNT/BC nanofiber nonwoven electrode exhibits larger specific capacitance up to 552.6 F g^{-1}, longer operation life with 95.6% capacitance retention after 5000 cycles, better conductivity with a fitting value of charge-transfer resistance of 9.87 Ω, outstanding flexibility and stability with specific capacitance retention over 96.4% after 1500 bending cycles. The remarkable electrochemical performance of PIn/CNT/BC nanofiber nonwoven electrode offer promising applications as flexible energy storage device for wearable and smart electronic components.

Keywords Polyindole · Carbon nanotubes · Bacterial cellulose · Nanofiber · Nonwoven electrode

Introduction

Nowadays, flexible electrodes have attracted more and more attention due to the development of wearable and smart electronics devices (Dubal et al. 2018; Jiang et al. 2017). A large and increasing amount of flexible electrodes are needed every year in the clothing industry, actuators, energy storage, electronics industry, especially the flexible supercapacitors (Despang et al. 2008; Alekseyev et al. 2018; Dong et al. 2017a, b; Choudhury et al. 2017; Saborío et al. 2018). Thus, a flexible electrode with high electrochemical performance, low environmental impact and favorable mechanical strength is desirable for practical applications. To approach this object, many efforts have been performed to fabricate paper electrodes, fiber electrodes, membrane electrodes and textile electrodes by

W. Jiajia · D. Zhanwen · X. Ping · C. Zhijiang (✉)
State Key Laboratory of Separation Membranes and Membrane Processes, School of Textiles Science and Engineering, Tiangong University, No 399 BingShuiXi Street, XiQing District, Tianjin 300387, China
e-mail: caizhijiang@hotmail.com

surface coating of active materials (Sundriyal and Bhattacharya 2017; Babu et al. 2018; Tian et al. 2017; Ankhili et al. 2018). Generally, transition metal oxides, conducting polymers and carbon materials are main active materials employed in electrode fabrication. Conducting polymers and carbon materials are more promising since the transition metal oxides are expensive and toxic. Many reports have focused on the development of conducting polymers based flexible electrodes using polyaniline (Dong et al. 2017a, b; Ma et al. 2018; Motlagh and Mottaghitalab 2017), polpyrrole (Gyurcsányi et al. 2015; Liang et al. 2013) or polythiophene (Li et al. 2016) as electrode active materials. However, few efforts have been made to explore the conducting polyindole based flexible electrodes. As one of the conducting polymers, polyindole possesses higher redox potential, better environmental stability and slower degradation rate compared with polyaniline, polpyrrole and polythiophene (Majumder et al. 2017; Tebyetekerwa et al. 2017; Chulliyote et al. 2017). It can be easily synthesized by electrochemical oxidation and radical polymerization. However, it is a challenge for pure conducting polymers to fabricate high performance flexible electrodes due to its low mechanical stability and flexibilty. Thus, carbon materials are selected to make composites with conducting polymers to improve its stability. Among various carbon materials, carbon nanotubes (CNTs) are the most attractive materials due to high specific surface areas, low electrical resistance, high stability and light weight. Polyaniline/CNT electrodes, polpyrrole/CNT electrodes and polythiophene/CNT electrodes have been reported and applied in supercapacitors, sensors and batteries (Malik et al. 2017; Oraon et al. 2017; Kumar et al. 2018; Thakur et al. 2017; Li et al. 2011; Shi & Zhitomirsky 2013; Maubane et al. 2012). In our previous work, some progress in polyindole/CNT electrodes has been obtained (Cai et al. 2016). But for the demands of flexible high performance electrodes, polyindole/CNT electrodes with highly stable structure still needs to be developed.

To fabricate flexible electrodes, a highly stable support material is need as substrate. Flexible substrates, such as thin metal foils, fabrics and polymer membranes, are mostly used (Dziedzic et al. 2017; Ge et al. 2019; Pendergraph et al. 2012; Yang et al. 2018; Peng et al. 2017). Among them, fabrics have the advantages of large specific surface areas, inherent flexibility, three-dimensional structure and wide availability. Xu et al. prepared a flexible composite electrode with hierarchical structure using non-woven fabric as substrate and reduced graphene oxide/carbon nanotubes/poly-3,4-ethylenedioxythiophene as active materials (Xu et al. 2018). Dong et al. demonstrated a flexible textile electrode with high-performance using activated carbon fiber cloth as body materials and CNTs as active materials (Dong et al. 2016). Lima et al. reported a multifunctional wearable electronic textiles using cotton fibers as substrate and polypyrrole/CNT composites as active materials (Lima et al. 2018).

In the present investigation, we developed a facile method to fabricate flexible PIn/CNT/BC nanofiber nonwoven electrode through a two-step process containing 'electrospinning & electrospray' process and potentiostatic polymerization. First, BC was selected as substrate materials because of its high mechanical properties as well as renewable natural polymer produced on industrial scales (Brandes et al. 2017; Gullo et al. 2017). While BC was electrospun into nanofiber nonwoven as a flexible framework, CNTs were electrosprayed onto BC nanofiber surface at the same time to form a conductive substance. Subsequently, PIn was deposited on the conductive substance by potentiostatic polymerization using D-tartaric acid (DTA) as dopant. The changes in surface morphology and structure of as-obtained flexible nonwoven electrode were investigated by SEM, TEM, BET and EDS measurements. The electrochemical performance of the flexible nonwoven electrode were characterized in terms of cyclic voltammetry, galvanostatic charge/discharge and electrochemical impedance spectroscopy.

Experiments

Indole monomer of chemical reagent grade was obtained from Bayer AG. Bacterial cellulose (BC) was kindly provided by Tianjin GreenBio Materials Co., Ltd. Single-wall Carbon nanotubes (CNTs) were purchased from Nanjing Xfnano Materials Tech Co., Ltd. D-tartaric acid and other chemicals were purchased from Tianjin KeLong Chemical Co., Ltd and used as received. Deionized water was used for all solution preparation.

To fabricate PIn/CNT/BC nonwoven electrode, a two-step process was employed as illustrated in Fig. 1. In step I, electrospinning and electrospray were performed simultaneously using rotate drum as collector. The details of the procedure were as following. BC was dissolved in trifluoroacetic acid to prepare 5.0 wt% spinning solution. The electrospinning process was carried out under applied high voltage of 25 kV, flow rate of 0.3 ml h^{-1} and collecting distance of 30 cm. CNTs were dispersed to prepare 1.0 wt% CNT aqueous solution. The electrospray process was performed under applied high voltage of 20 kV, flow rate of 3 ml h^{-1} and collecting distance of 10 cm. In step II, polyindole was deposited on the surface of BC/CNT nanofibers by potentiostatic polymerization using a Potentiostat controlled by computer (Electrochemical workstation, Solartron 1287, UK). During the potentiostatic polymerization process, BC/CNT nanofibers were used as working electrode, Pt gauge and saturated calomel electrode (SCE) were used as counter electrode and reference electrode, respectively. An aqueous solution containing 0.2 mol h^{-1} indole and 0.1 mol h^{-1} D-tartaric acid was used as electrolyte. The potentiostatic polymerization was carried out at 1.0 V for 120 min. After polymerization, it was washed by water three times and dried in vacuum overnight.

A Transmission Electronic Microscopy (TEM, JEM-1200EX, Japan) and a Scanning Electronic Microscopy (SEM, Hitachi S-4200, Japan) equipped with energy dispersive spectroscopy (EDS) analysis were used to investigate the surface morphology and elements content of the samples. A Perkin Elmer Spectra 2000 FTIR spectrometer was applied to characterize the composition of the samples. The test was carried out in the range of 4000–800 cm^{-1} at 5 cm^{-1} resolution. A Sorptomatic-1990 surface area analyzer was employed to measure the specific surface areas of the samples by the Brunauer–Emmett–Teller (BET) method.

The electrochemical performance of the flexible electrode in terms of cyclic voltammetry (CV), galvanostatic charge–discharge (GCD), and electrochemical impedance spectroscopy (EIS) were carried out on the electrochemical workstation (Solartron 1287, UK) in three-electrode configuration system. The flexible PIn/CNT/BC nanofiber electrode, Pt gauge and saturated calomel electrode (SCE) were used as working electrode, counter electrode and reference electrode, respectively. 1 mol l^{-1} D-tartaric
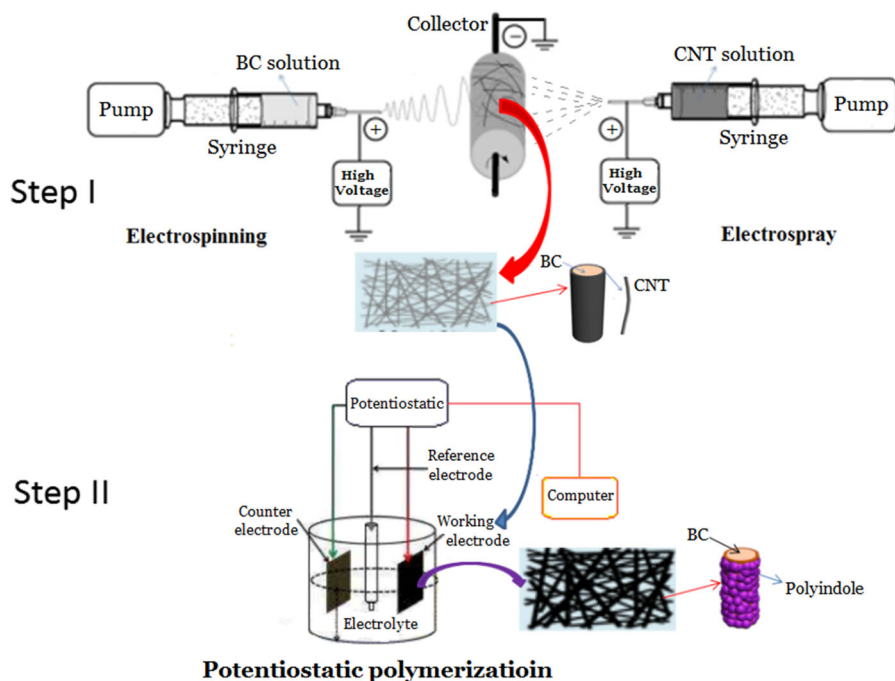

Fig. 1 Schematic preparation process of PIn/CNT/BC nanofiber nonwoven electrode

acid aqueous solution was used as electrolyte. CV tests were carried out with the applied voltage ranged from 0 to 1.0 V at various scan rate in the range of 10–50 mV s^{-1}. GCD measurements were performed at current density ranged from 10 to 200 mA cm^{-2} within the potential window of 0 to 1.2 V by galvanostatic cycler. EIS was recorded at open circuit voltage with 5 mV AC amplitude with the applied frequency ranged from 0.01 Hz to 100 kHz.

Results and discussion

Surface morphology

Figure 2 presents the SEM images and fiber diameter distribution of as-obtained PIn/CNT/BC nanofiber nonwoven electrode in comparison with pure BC and BC/CNT nanofiber nonwoven. During the 'electrospinning and electrospray' process, BC is electrospun into nanofiber nonwoven (Fig. 2a) with average diameter of 195 ± 65 nm (Fig. 2d) and the CNTs are uniformly coated on the surface of BC nanofibers at the same time. Thus, a three-dimensional conductive network consisting of CNT layer (Fig. 2g) can be formed for BC/CNT nonwoven with average diameter increased to 244 ± 86 nm (Fig. 2b, e). Besides, new 'sprout' structure is generated on the smooth surface of BC nanofibers (Fig. 2) due to aggregation of CNTs, resulting in improvement of specific surface areas with value increased from 76.21 m^2 g^{-1} for pure BC nanofibers to 81.44 m^2 g^{-1}. During potentiostatic polymerization, indole is electrochemical synthesized and deposited along the BC/CNT nanofibers (Fig. 2c). It is clear that BC/CNT nanofibers have been uniformly covered by PIn nanoparticles, forming a broccoli-like rough surface with higher specific surface area (114.72 m^2 g^{-1}) of electrode as shown in Fig. 2c. Using this two-step process, a hierarchy configuration can be fabricated containing BC electrospun nanofibers, CNT coating layer and PIn nanoparticle electrode layer, which play the function of supporting substrate, conductive path and electrode active material, respectively.

Table 1 summarizes the average fiber diameter and specific surface areas of pure BC, BC/CNT and PIn/CNT/BC nonwoven electrode. PIn nanoparticles incorporation can greatly improve specific surface areas by 50% to 114.72 m^2 g^{-1} with average fiber

diameter increased by 44% to 283 nm. Compared with SEM and TEM images, the thickness of CNT coating layer on BC nanofibers is about 25 nm, which is dependent on concentration of CNT aqueous solution. The size of PIn nanoparticles is about 20 nm, which is related with indole concentration and potentiostatic polymerization parameters. This PIn/CNT/BC nanofiber nonwoven electrode is more suitable as flexible electrode for supercapacitor applications. The electrospun BC nanofiber nonwoven as supporting substrate can give the electrode flexible and strength. The CNT coating layer as conductive path can greatly reduce the diffusion resistance of the electrolyte into electrode matrix. The PIn nanoparticle electrode layer with huge specific surface areas can provide more site for electrochemical reaction and will lead to high specific capacitance.

FT-IR analysis

Figure 3a depicts the FTIR spectra of PIn/CNT/BC nanofiber nonwoven electrode compared with BC/CNT nonwoven. As seen the curve for BC/CNT, the strong adsorption peak detected at 1080 cm^{-1} is assigned to the C–O–C stretching vibrations of BC characteristic adsorption peak. The broad peak located at 3433 cm^{-1} is due to the characteristic stretching vibrations of O–H bond existed in BC and CNTs (Sarı et al. 2017). The adsorption peaks observed at 2935 cm^{-1} and 940 cm^{-1} are ascribed to the C–H stretching vibration and in-plane deformation. A sharp peak at 1755 cm^{-1} is marked by the C=O characteristic stretching vibration, which might be formed by the molecular interaction between the –OH of BC and –COOH of CNTs. For PIn/CNT/BC curve, the new adsorption peak at 1582 cm^{-1} is assigned to the characteristic stretching and deformation vibrations of N–H bond. The adsorption peak at 1270 and 1205 cm^{-1} are the heterocyclic ring stretching modes and stretching mode of C$_8$–N–C$_2$–C$_3$ group on indole ring. The adsorption peak at 1180 cm^{-1} signifies the C–N bond vibration modes. Adsorption peaks at 750 cm^{-1} and 780 cm^{-1} are ascribed to the characteristic stretching modes of benzene ring in polyindole and C–H bond out-of-plane deformation of polyindole (Cai et al. 2012). In addition, the peak located at 3433 cm^{-1} becomes broader and stronger and the wavenumber is shifted to 3400 cm^{-1} due to hydrogen-bonded N–H stretching vibration in the D-tartaric acid

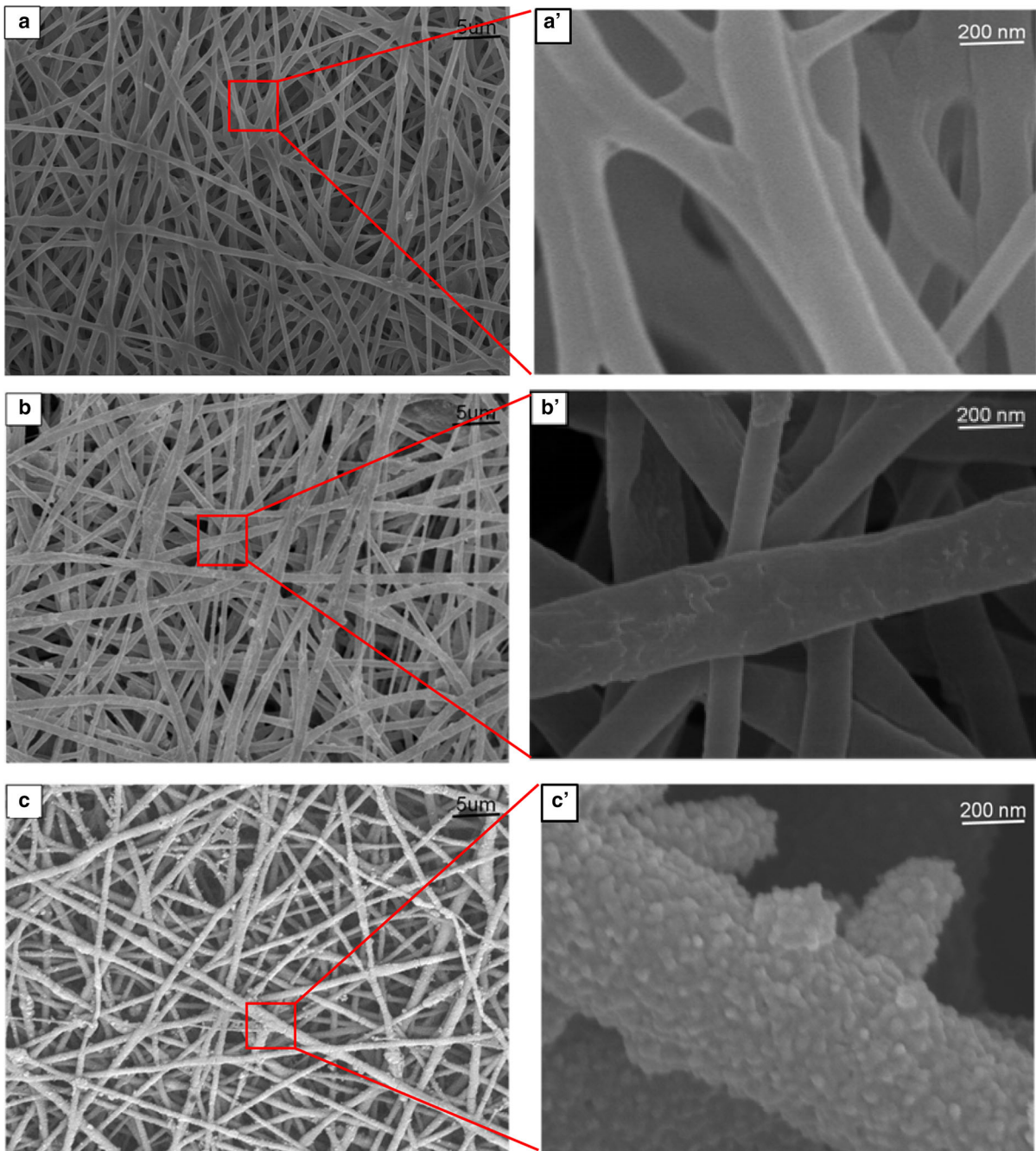**Fig. 2** The SEM images of pure BC (**a, a'**), BC/CNT (**b, b'**) and PIn/CNT/BC (**c, c'**) nanofiber nonwoven; the fiber diameter distribution of pure BC (**d**), BC/CNT (**e**) and PIn/CNT/BC (**f**) nanofiber nonwoven; TEM image of PIn/CNT/BC nanofiber nonwoven electrode (**g**)

doped polyindole. An extra new adsorption peak observed at 1680 cm^{-1} is due to the C=O asymmetric stretching vibration band in D-tartaric acid (Zhong et al. 2006). These evidences suggest that the D-

tartaric acid enters the polyindole as dopant ions via hydrogen bonding. At the same time, it can be confirmed that that polyindole doped with D-tartaric
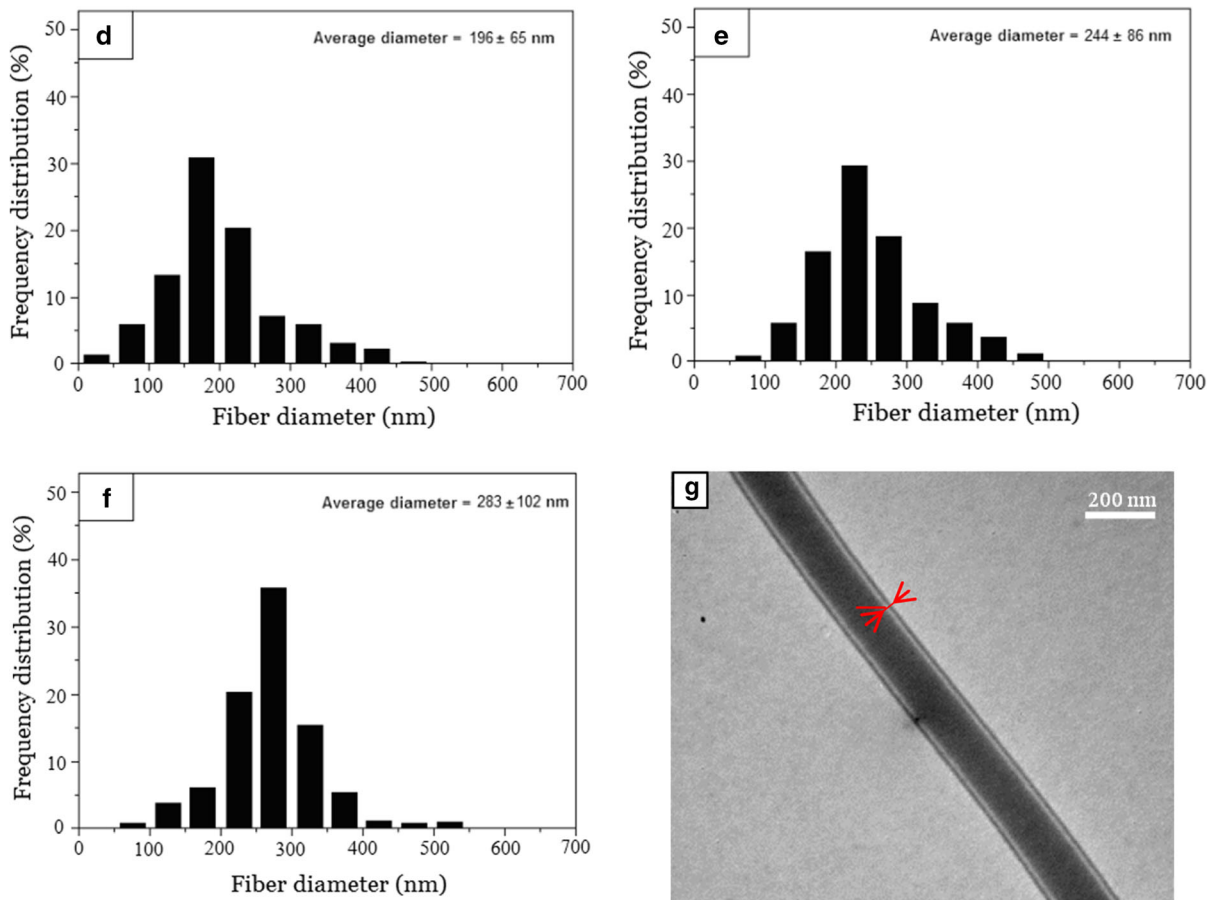
Fig. 2 continued

Table 1 Physical properties of the PIn/CNT/BC electrode compared with pure BC and BC/CNT nonwoven

	Average fiber diameter (nm)	BET surface areas ($m^2\ g^{-1}$)
BC	196 ± 65	76.21 ± 8.81
BC/CNT	244 ± 86	81.44 ± 9.23
PIn/CNT/BC	283 ± 102	114.72 ± 12.51

acid was coated on the surface of BC/CNT nanofibers forming PIn/CNT/BC nanofiber nonwoven electrode.

EDS analysis

Figure 3b shows the EDS spectra of BC/CNT and PIn/CNT/BC nanofiber nonwoven electrode. Using EDS spectra, the surface elemental contents of carbon (C), hydrogen (H), and nitrogen (N) for BC/CNT and PIn/CNT/BC nanofiber nonwoven electrode can be analyzed. For BC/CNT, two peaks corresponded to C and O element can be detected due to its chemical unit structure as illustrated in inset of Fig. 3b. It contains 78.4% C and 21.6% O. For PIn/CNT/BC, a new adsorption peak located at 0.394 keV, which is contributed to the characteristic peak of N atom, can be observed. PIn/CNT/BC contains 63.2% C, 29.3% O, and 7.5% N (Table 2). Since N atom is only originated from PIn, the result chemically confirms
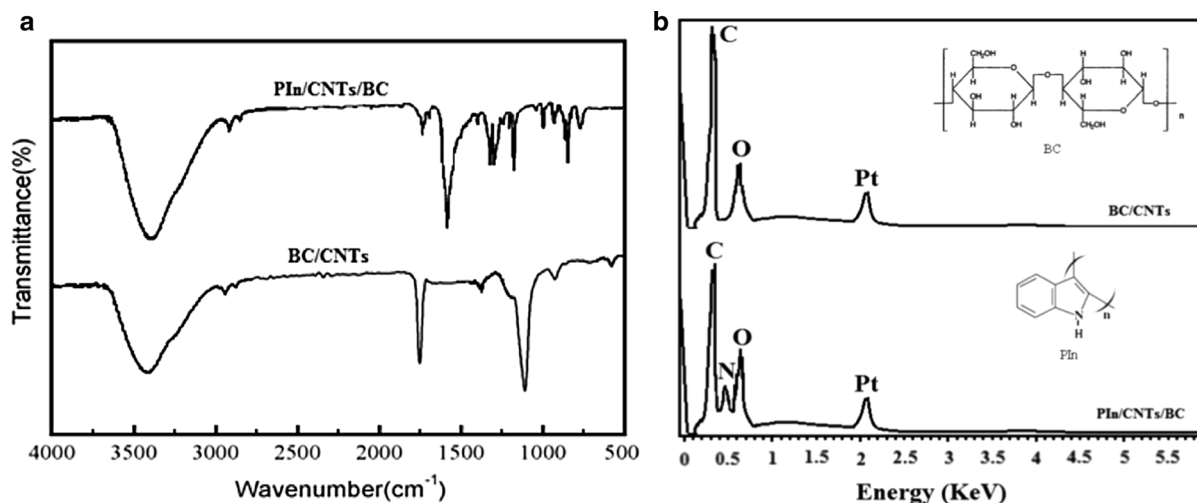
Fig. 3 The FTIR (**a**) and EDS (**b**) spectra of BC/CNT and PIn/CNT/BC nanofiber nonwoven electrode (Inset: chemical unit structure of BC and PIn)

Table 2 The amount of C, O and N elements on the surface of BC/CNT and PIn/CNT/BC nanofiber nonwoven electrode by EDS analysis

	Surface elemental content (%)			
	C	O	N	Total
BC/CNT nonwoven	78.4 ± 0.71	21.6 ± 0.33	0	100
PIn/CNT/BC nonwoven electrode	63.2 ± 0.57	29.3 ± 0.41	7.5 ± 0.11	100

that PIn has been incorporated on BC/CNT forming PIn/CNT/BC nanofiber nonwoven electrode.

Cyclic voltammogram

The electrochemical performance of the flexible PIn/CNT/BC nanofiber nonwoven electrode were evaluated in 1 mol l^{-1} D-tartaric acid electrolyte. Figure 4a presents the CV curve of PIn/CNT/BC electrode compared with BC/CNT at a scan rate of 0.1 V s^{-1}. The CV curve of BC/CNT has the parallelogram curve shape indicating the double layer and ideal capacitive behavior of CNTs. Whereas, a couple of redox peaks are detected in the PIn/CNT/BC electrode CV curves. The anodic peak and cathodic peak are associated with the doping/de-doping of PIn. Obviously, the PIn/CNT/BC electrode shows higher capacitance in comparison with BC/CNT electrode, resulting from the highly electrochemical activity of PIn nanoparticles deposited on the BC/CNT surface.

In addition, the hierarchy configuration of PIn/CNT/BC electrode can provide larger specific surface area, highly conducting path and 3D network structure for ion insertion and extraction, leading to improvement of capacitance for PIn/CNT/BC nanofiber nonwoven electrode.

Figure 4b shows the CV curves of the PIn/CNT/BC nonwoven electrode at various scan rate ranged from 0.05 to 0.5 V s^{-1}. The oxidation peaks are at around 0.6 V and the reduction peaks are approximately 0.3 V at various scan rates, which is associated with the DTA ions doping/de-doping into PIn in the DTA aqueous solution by oxidation and reduction reactions as expressed as in Fig. 4c. With the scan rate increasing, the anodic peaks are shifted to positive region and the cathodic peaks are shifted to negative region. These behaviors also confirm that PIn has been deposited on BC/CNT surface.

Figure 4d demonstrates the CV curves of PIn/CNT/BC nonwoven electrode for 5000 cycles at a scan rate
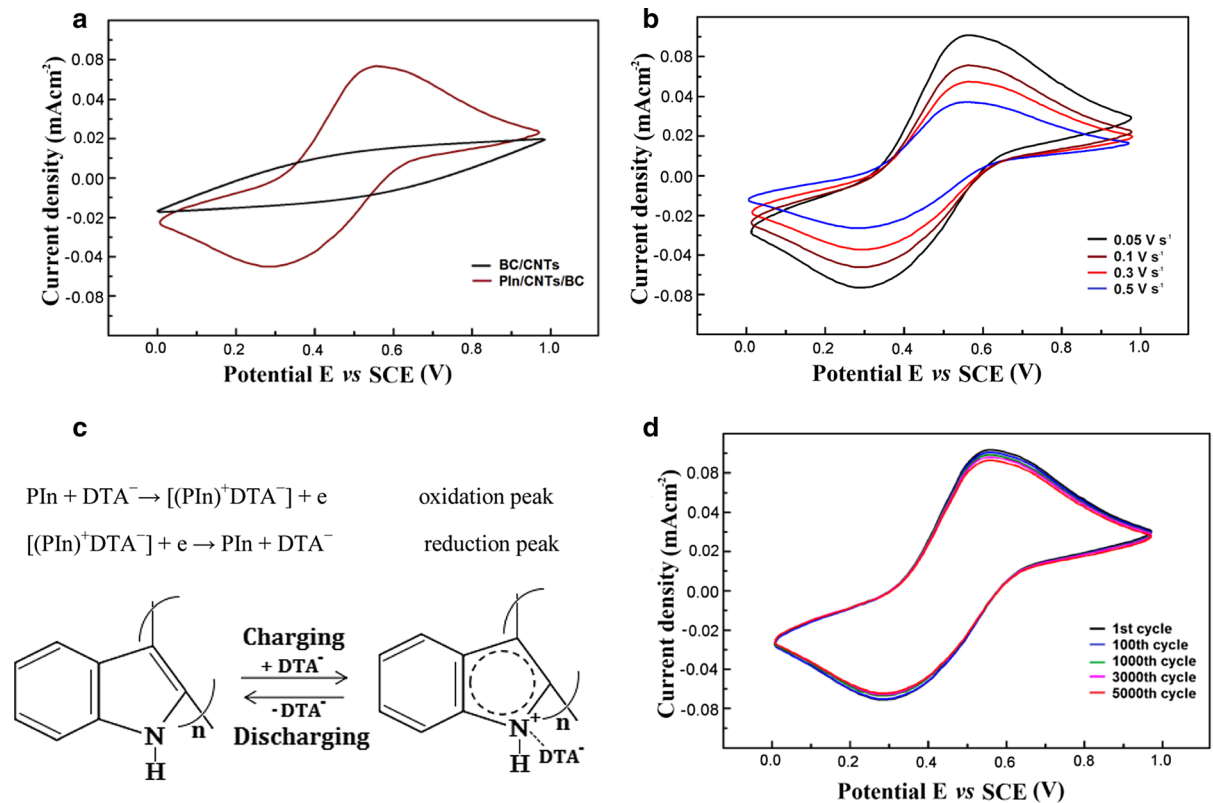
Fig. 4 The CV curves of BC/CNT and PIn/CNT/BC nonwoven electrode compared at a scan rate of 0.1 V s^{-1} (**a**); the CV curves of PIn/CNT/BC nanofiber nonwoven electrode at various of 0.05 V s^{-1}. After 5000 cycles, the decay of the integral area of the CV loop is negligible. The retention of the specific capacitance calculated from the area of CV loop is about 96.7%, which indicate excellent stability of the PIn/CNT/BC nonwoven electrode.

scan rate (**b**); the doping/de-doping process of DTA ions into PIn (**c**); and the CV curves of PIn/CNT/BC nanofiber nonwoven electrode for 5000 cycles at a scan rate of 0.05 V s^{-1} (**d**)

Nyquist plots

The charge-transfer resistance (R_{ct}) and electrode resistance (R_Ω) performance of nonwoven electrodes were characterized by EIS test with the frequency ranged from 0.01 Hz to 100 KHz and AC voltage amplitude of 5 mV. Figure 5a illustrates the test results of Nyquist plots for the PIn/CNT/BC nonwoven electrode in comparison with BC/CNT electrode. Nyquist impedance plot of PIn/CNT/BC nonwoven electrode shows a compressed semicircle over the high-frequency region and a near vertical line over the low-frequency region. Generally, the diameter of the

compressed semicircle in the high-frequency range is related to the R_{ct}, which is associated with the charge transfer reaction at the electrolyte/electrode interface in the electrochemical system. The slope of the vertical line in the low-frequency range is related to the R_Ω, which is associated with the ion diffusion process in the electrodes (Liu et al. 2009). As seen from the Nyquist plot of BC/CNT electrode, only vertical line without semicircle can be observed from high to low frequency range. This result indicates that only ions diffusion are involved during the electrochemical process. Whereas, the R_{ct} determined by the semicircle diameter at the high-frequency range is about 9.87 Ω and the R_Ω obtained from the nearly linear spike in the low frequency region is about 0.33 Ω for the PIn/CNT/BC nonwoven electrode, respectively. The R_{ct} of PIn/CNT/BC nonwoven electrode is much smaller than the values of polyindole/CNT electrode (Cai et al. 2016), indicating higher conductive capability. The reason might be attributed to the
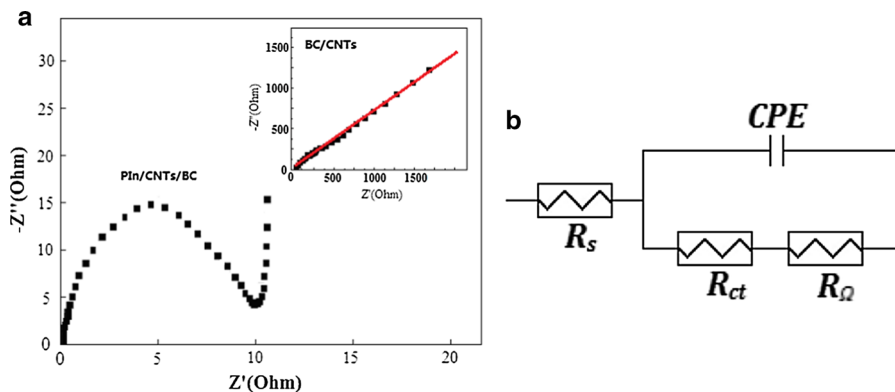
Fig. 5 The electrochemical impedance spectra of BC/CNT and PIn/CNT/BC nanofiber nonwoven electrode (**a**); the electrical equivalent circuits of PIn/CNT/BC nanofiber nonwoven electrode (**b**)

fact that nanofibrious structure formed in the nanofibers can help to facilitate the fast diffusion of electrolyte ions into composite nanofiber electrode.

Figure 5b demonstrate the equivalent circuit model for the PIn/CNT/BC nonwoven electrode. The circuit elements include R_{ct} (charge-transfer resistance, equal to the diameter of the semicircle), R_Ω (electrode resistance, the slope of the vertical line), R_s (electrolyte resistance, equivalent to the high-frequency intercept on the real axis) and *CPE* (constant phase element for double layer capacitance) (Xu et al. 2014).

Galvanostatic charge–discharge performance

Galvanostatic charge–discharge (GCD) tests are carried out to evaluate the electrochemical properties of nanofiber nonwoven electrodes. Figure 6a, b present the GCD curves of BC/CNT and PIn/CNT/BC nonwoven electrodes performed at various current density with the potential window between 0.0 and 1.2 V. The specific capacitance (C_p) can be calculated from the GCD curves using the following equation.

$$C_p = \frac{I \times t}{\Delta V \times m} \tag{1}$$

where I and t mean the discharge current (A) and discharge time (s), ΔV and m are the potential window (V) and mass of active material in electrode (g).

As seen from the Fig. 6a, the GCD curves of BC/CNT at various current density display nearly symmetrical shapes, which indicates double layer capacitive behavior. For PIn/CNT/BC nonwoven electrode, the GCD curves are not symmetrical shapes because of the redox reaction of PIn (Fig. 6b). The discharge

curves are nearly symmetrical to charge curves with a small voltage drop, suggesting small internal resistance and good capacitive behavior of the PIn/CNT/BC nonwoven electrode. Obviously, the discharge time of the PIn/CNT/BC electrode is much longer than that of BC/CNT electrode, indicating higher charge storage capability of PIn/CNT/BC electrode, which is consistent with the CV test results. At a low current density of 10 mA cm^{-2}, the C_p of BC/CNT and PIn/CNT/BC electrodes reach to about 4.7 F g^{-1} and 552.6 F g^{-1}, respectively. With current density increasing to 50 and 200 mA cm^{-2}, the C_p remains about 3.6 and 2.1 F g^{-1} for BC/CNT, 375.1 and 203.5 F g^{-1} for PIn/CNT/BC, respectively. These values are almost as ten times as the C_p of BC/CNT electrode and higher than that of polyaniline nanofiber electrode (Liu et al. 2015; Yang et al. 2013) and polypyrrole electrode (Kim et al. 2008; Lota et al. 2015). The enhanced C_p might be due to high specific surface area of PIn nanoparticles, providing large open areas between the electrolyte and the electrode. In addition, the PIn as a conductive polymer can provide pseudo-capacitance to a great extent for energy storage.

Specific energy and power

The specific energy (E_s, Wh kg^{-1}) and specific power (P_s, W kg^{-1}) were also calculated from the following equations using GCD curves to evaluate the electrochemical performance of the flexible nanofiber nonwoven electrodes.
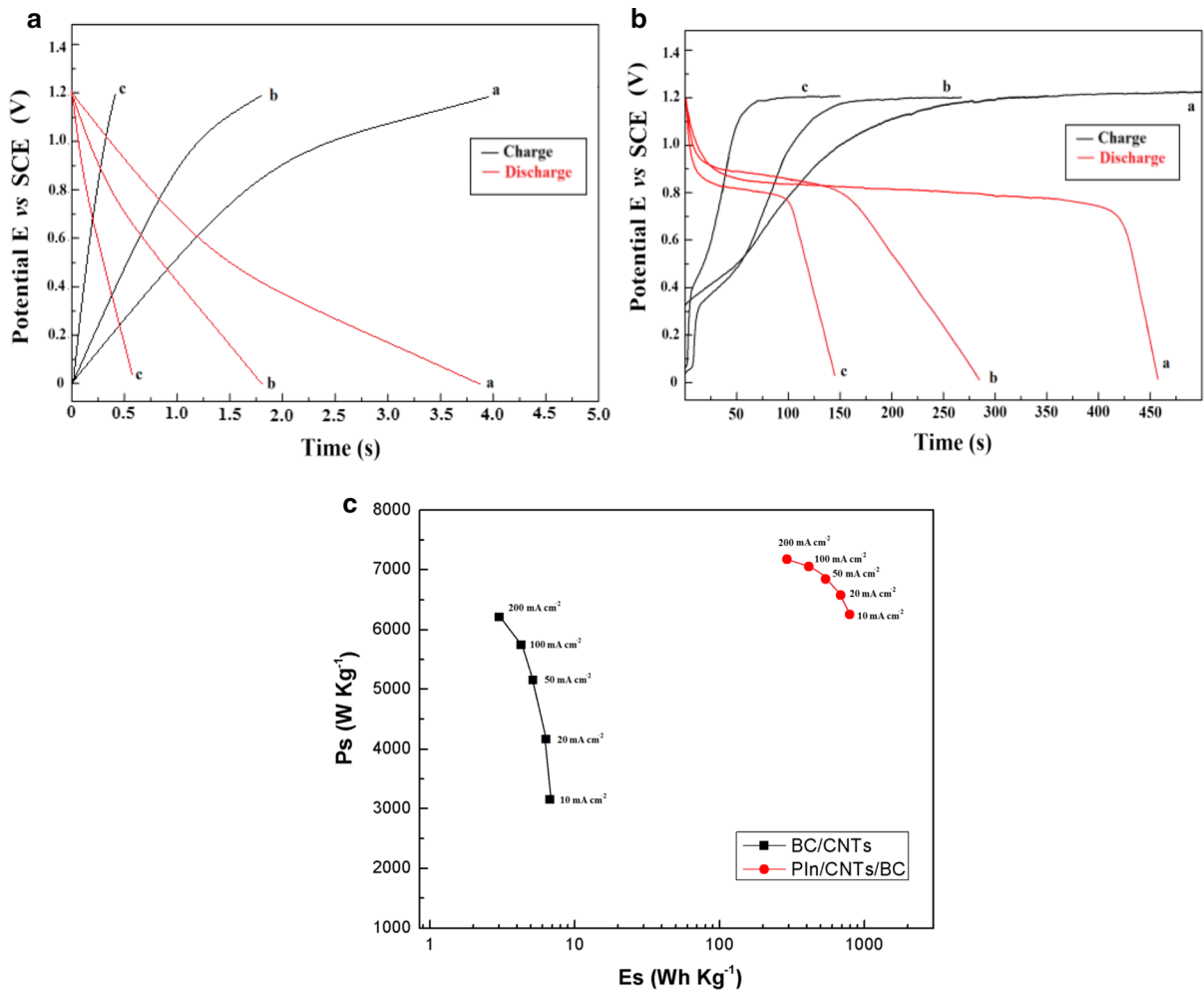
Fig. 6 The GCD curves of BC/CNT (**A**) and PIn/CNT/BC (**B**) nanofiber nonwoven electrodes at various current density (a: 10 mA cm^{-2}; b: 50 mA cm^{-2}; c: 200 mA cm^{-2}); Ragon plots for BC/CNT and PIn/CNT/BC nanofiber nonwoven electrodes (**C**)

$$E_s = \frac{I \times \Delta V \times t}{m} \qquad (2)$$

$$P_s = \frac{I \times \Delta V}{m} \qquad (3)$$

Figure 6C demonstrates the resultant Ragon plots for BC/CNT and PIn/CNT/BC electrodes at various current density ranged from 10 to 200 mA cm^{-2}. For both BC/CNT and PIn/CNT/BC electrodes, the specific power gradually increases with the increase of current density, while the specific energy decreases with the increase of current density. PIn/CNT/BC electrode has higher E_s and P_s than BC/CNT electrode. At the same P_s, the E_s of PIn/CNT/BC electrode is two orders of magnitude larger than that of BC/CNT

electrode. The reason may be due to the the hierarchy configuration with nano-sized structure of PIn/CNT/BC nanofiber nonwoven electrode which can offer excellent conductive path and large quantity of charge passways. The PIn nanoparticles acted as active materials provide more electrode—electrolyte interface areas, which can facilitate faradaic reactions.

Stability and reversibility

The long-term cycle stability and reversibility of the PIn/CNT/BC nanofiber nonwoven electrode are key factor which affect its practical applications. The cycle stability test was carried out by GCD test at a current density of 10 mA cm^{-2} for 5000 cycles, as shown in
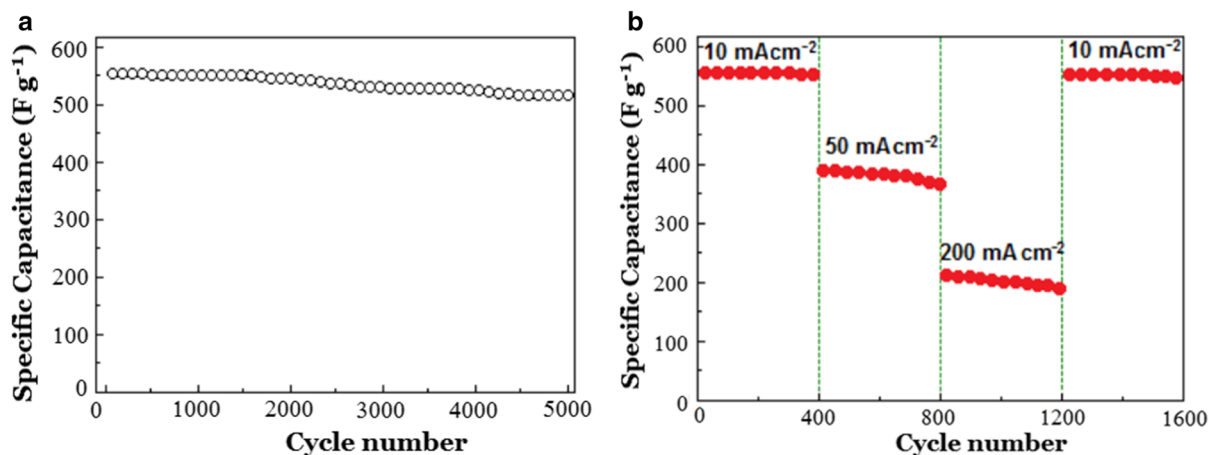
Fig. 7 The cycle stability of PIn/CNT/BC nanofiber nonwoven electrode for 5000 cycles (**a**) and the reversible capacitance of the PIn/CNT/BC electrode for 1600 cycles (**b**)

Fig. 7a. The specific capacitance of the PIn/CNT/BC electrode still can keep at 517.6 F g^{-1}, which is about 95.6% of initial value after 5000 charge–discharge cycles. This result indicates that PIn/CNT/BC nanofiber nonwoven electrode has excellent stability for a long cycle life, which is consistent with the CV test results. The reversibility of the PIn/CNT/BC nanofiber nonwoven electrode was performed by GCD test with current density progressively increased from 10 to 50 and 200 mA cm^{-2} for 400 cycles, respectively. After continuous 1200 cycles, the current density was decreased back to 10 mA cm^{-2} for another 400 cycles. The reversible capacitance of the PIn/CNT/BC electrode could recover about 98.2% of the value compared with the first cycle at current density of 10 mA cm^{-2}, as depicted in Fig. 7b. The excellent stability and reversibility of PIn/CNT/BC electrode might be attributed to the hierarchy configuration composed by BC nanofibers and PIn nanoparticles. This submicro/nano-sized composite structure has good tolerance during the charge–discharge process. The PIn/CNT/BC electrode with superior electrochemical properties may have promising applications in supercapacitor.

Flexibility

As a flexible electrode, the electrochemical performance under mechanical bending are very important for practical applications. Thus, the PIn/CNT/BC nanofiber nonwoven electrode is bent at 90°and

180°for electrochemical tests. The results are shown in Fig. 8 in comparison with the electrode at original state (0°). When the electrode is bent at 90° and 180°, the CV curves keep almost the same shape without any conspicuous deviation (Fig. 8a). The specific capacitance calculated from the area of CV loop decreases by 1.1% and 1.4%, respectively (Fig. 8b). Moreover, the electrode shows about 96.4% specific capacitance retention after 1500 cycles of bending (Fig. 8c, d). The capacitance decays with bending might be due to nanofiber break and PIn nanoparticle drop off from nanofiber surface in the local areas. However, this value is better than the previously reported polyaniline/CNT film electrode (92% after 300 cycles of bending) and polyaniline/CNT coated plastic fiber electrode (94% after 1000 cycles of bending) (Liu et al. 2017; Miao et al. 2016), suggesting excellent flexibility of the PIn/CNT/BC nanofiber nonwoven electrode. Therefore, the PIn/CNT/BC nanofiber nonwoven electrode is ideal electrode material for energy storage devices for wearable and smart electronic applications.

Conclusions

In the present study, a facile two-step method was adopted to fabricate the flexible PIn/CNT/BC nanofiber nonwoven electrode with a broccoli-like rough surface generated by polyindole nanoparticles. The PIn/CNT/BC nanofiber nonwoven electrode shows
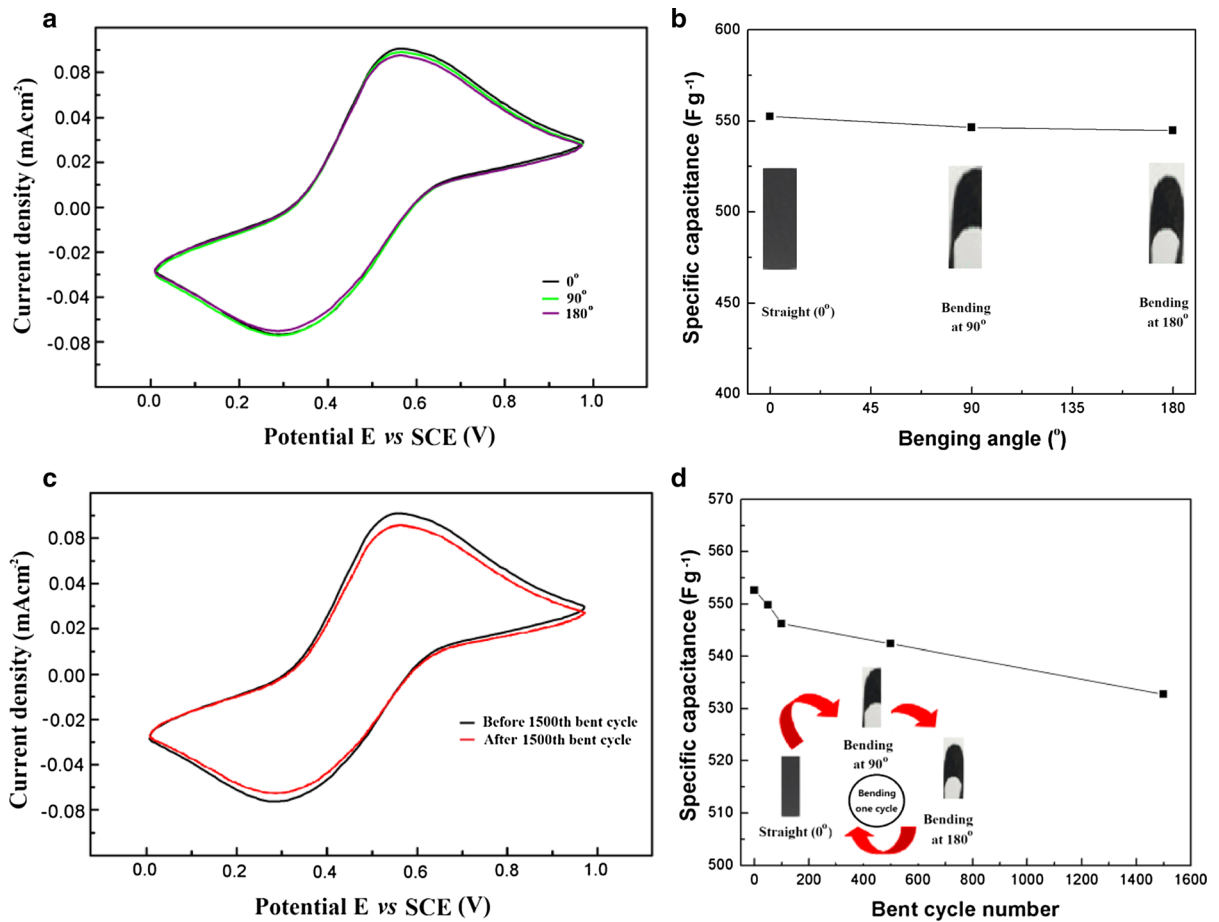
Fig. 8 The CV curves (**a**) and specific capacitance (**b**) of PIn/CNT/BC nanofiber nonwoven electrode bending at various angle; the CV curves of PIn/CNT/BC nanofiber nonwoven electrode before and after 1500 bent cycles (**c**); specific capacitance with bent cycle number (**d**)

better electrochemical performance with a specific capacitance of 552.6 F g^{-1} and a value of R_{ct} of 9.87 Ω. In addition, the PIn/CNT/BC nanofiber nonwoven electrode possesses a long operation life and outstanding flexibility. As we expected, the improved electrochemical performance are not only due to the high electrical activity of PIn nanoparticles deposited on the surface of electrode, but also ascribed to the three-dimensional hierarchical network structure for effective charge transfer. Thus, the as-obtained flexible PIn/CNT/BC nanofiber nonwoven electrode might have promising potentials for wearable and smart electronics devices.

Compliance with ethical standards

Conflict of interest The authors declare that they have no conflict of interest.

References

Alekseyev NI, Broyko AP, Kalyonov VE, Korlyakov AV, Lagosh AV, Livshits AO et al (2018) The structure of silver modified flexible graphene electrodes for actuators in biomimetic systems. J Struct Chem 59(4):891–899

Ankhili A, Tao X, Cochrane C, Coulon D, Koncar V (2018) Washable and reliable textile electrodes embedded into underwear fabric for electrocardiography (ecg) monitoring. Materials 11(2):256. https://doi.org/10.3390/ma11020256

Babu RS, Barros ALFD, Maier MDA, Sampaio DDM, Balamurugan J, Lee JH (2018) Novel polyaniline/manganese hexacyanoferrate nanoparticles on carbon fiber as binder-free electrode for flexible supercapacitors. Compos B Eng 143:141–147

Brandes R, Carminatti C, Mikowski A, Al-Qureshi H, Recouvreux D (2017) A mini-review on the progress of spherical bacterial cellulose production. J Nano Res 45:142–154

Cai Z, Zhang R, Shi X (2012) Preparation and characterization of polyindole nanofibers by electrospinning method. Synth Met 162(23):2069–2074

Cai ZJ, Zhang Q, Song XY (2016) Improved electrochemical performance of polyindole/carbon nanotubes composite as electrode material for supercapacitors. Electron Mater Lett 12(6):1–11

Choudhury A, Kim JH, Mahapatra SS, Yang KS, Yang DJ (2017) Nitrogen-enriched porous carbon nanofiber mat as efficient flexible electrode material for supercapacitors. ACS Sustain Chem Eng 5(3):2109–2118

Chulliyote R, Hareendrakrishnakumar H, Raja M, Gladis JM, Stephan AM (2017) Enhanced cyclability using a polyindole modified cathode material for lithium sulphur batteries. Sustain Energy Fuels 1(8):1774–1781

Despang HG, Netz S, Heinig A, Holland HJ, Fischer WJ (2008) Wireless long-term ecg integrated into clothing. Biomed Eng-Biomedizinische Technik 53(6):270–278

Dong L, Liang G, Xu C, Liu W, Pan ZZ, Zhou E et al (2017a) Multi hierarchical construction-induced superior capacitive performances of flexible electrodes for wearable energy storage. Nano Energy 34:242–248

Dong L, Liang G, Xu C, Ren D, Wang J, Pan ZZ et al (2017b) Stacking up layers of polyaniline/carbon nanotube networks inside papers as highly flexible electrodes with large areal capacitance and superior rate capability. J Mater Chem A 5(37):19934–19942

Dong L, Xu C, Li Y, Wu C, Jiang B, Yang Q et al (2016) Simultaneous production of high-performance flexible textile electrodes and fiber electrodes for wearable energy storage. Adv Mater 28(8):1675–1681

Dubal DP, Chodankar NR, Kim DH, Gomez-Romero P (2018) Towards flexible solid-state supercapacitors for smart and wearable electronics. Chem Soc Rev 47(39):2065–2081

Dziedzic A, Osypiuk P, Steplewski W (2017) Stability of electrical properties for mechanically exposed thick- and thin-film resistors on flexible substrates. Solder Surf Mt Technol 29(1):54–58

Ge F, Chen Y, Liu A, Guang S, Cai Z (2019) Flexible and recyclable sers substrate fabricated by decorated tio 2 film with ag nps on the cotton fabric. Cellulose 26(4):2689–2697

Gullo M, Sola A, Zanichelli G, Montorsi M, Messori M, Giudici P (2017) Increased production of bacterial cellulose as starting point for scaled-up applications. Appl Microbiol Biotechnol 101(22):8115–8127

Gyurcsányi RE, Nybäck AS, Ivaska A, Tóth K, Nagy G (2015) Novel polypyrrole based all-solid-state potassium-selective microelectrodes. Analyst 123(6):1339–1344

Jiang H, Wang H, Liu G, Su Z, Wu J, Liu J et al (2017) Lightweight, flexible, low-voltage electro-thermal film using graphite nanoplatelets for wearable/smart electronics and deicing devices. J Alloy Compd 699:1049–1056

Kim JY, Kim KH, Kim KB (2008) Fabrication and electrochemical properties of carbon nanotube/polypyrrole composite film electrodes with controlled pore size. J Power Sour 176(1):396–402

Kumar N, Sahoo PK, Panda HS (2018) Localize current burst in modified carbon nanotube/polyaniline composite fibers mat electrode miniaturized resistance and improved rate

capability for solid-state supercapacitor. J Mater Sci: Mater Electron 1:1–13

Li CT, Lee CT, Li SR, Lee CP, Chiu IT, Vittal R et al (2016) Composite films of carbon black nanoparticles and sulfonated-polythiophene as flexible counter electrodes for dye-sensitized solar cells. J Power Sour 302(4):155–163

Li J, Liu Y, Wei W, Luo S (2011) Fabrication of tiron doped poly-pyrrole/carbon nanotubes on low resistance monolayer-modified glassy carbon electrode for selective determination of dopamine. Anal Lett 44(7):1226–1240

Liang G, Zhu L, Jie X, Dong F, Bai Z, Xu W (2013) Investigations of poly(pyrrole)-coated cotton fabrics prepared in blends of anionic and cationic surfactants as flexible electrode. Electrochim Acta 103(8):9–14

Lima RMAP, Espinoza A, Jarib J, Da Silva FAG, De Oliveira HP (2018) Multifunctional wearable electronic textiles using cotton fibers with polypyrrole and carbon nanotubes. ACS Appl Mater Interfaces 10(16):13783–13795

Liu F, Luo S, Dong L, Wei C, Yang H, Lei D et al (2017) Facile processing of free-standing polyaniline/SWCNT film as an integrated electrode for flexible supercapacitor application. ACS Appl Mater Interfaces 9(39):33791–33801

Liu H, Xu B, Jia M, Mei Z, Cao B, Zhao X et al (2015) Polyaniline nanofiber/large mesoporous carbon composites as electrode materials for supercapacitors. Appl Surf Sci 332:40–46

Liu Y, Zhou X, Guo Y (2009) Effects of fluorine doping on the electrochemical properties of LiV_3O_8 cathode material. Electrochim Acta 54:3184–3190

Lota K, Lota G, Sierczynska A, Acznik I (2015) Carbon/polypyrrole composites for electrochemical capacitors. Synth Met 203:44–48

Ma J, Tang S, Syed JA, Su D, Meng X (2018) High-performance asymmetric supercapacitors based on reduced graphene oxide/polyaniline composite electrodes with sandwich-like structure. J Mater Sci Technol 34(7):45–51

Malik R, Zhang L, Mcconnell C, Schott M, Hsieh YY, Noga R et al (2017) Three-dimensional, free-standing polyaniline/carbon nanotube composite-based electrode for high-performance supercapacitors. Carbon 116:579–590

Majumder M, Choudhary RB, Koiry SP, Thakur AK, Kumar U (2017) Gravimetric and volumetric capacitive performance of polyindole/carbon black/mos 2 hybrid electrode material for supercapacitor applications. Electrochim Acta 248:98–111

Maubane MS, Mamo MA, Nxumalo EN, Otterlo WALV, Coville NJ (2012) Tubular shaped composites made from polythiophene covalently linked to prato functionalized n-doped carbon nanotubes. Synth Met 162(24):2307–2315

Miao F, Shao C, Li X, Wang K, Lu N, Liu Y (2016) Electrospun carbon nanofibers/carbon nanotubes/polyaniline ternary composites with enhanced electrochemical performance for flexible solid-state supercapacitors. ACS Sustain Chem Eng 43:1689–1696

Motlagh MS, Mottaghitalab V (2017) The charge transport characterization of the polyaniline coated carbon fabric as a novel textile based counter electrode for flexible dye-sensitized solar cell. Electrochim Acta 249:308–317

Oraon R, Adhikari AD, Tiwari SK, Nayak GC (2017) Nanoclay co–doped cnt/polyaniline nanocomposite: a high-

performance electrode material for supercapacitor applications. Chemistryselect 2(28):8807–8817

Pendergraph SA, Bartlett MD, Carter KR, Crosby AJ (2012) Opportunities with fabric composites as unique flexible substrates. ACS Appl Mater Interfaces 4(12):6640–6645

Peng S, Fan L, Rao W, Bai Z, Xu W, Jie X (2017) Bacterial cellulose membranes coated by polypyrrole/copper oxide as flexible supercapacitor electrodes. J Mater Sci 52(4):1930–1942

Sarı A, Bicer A, Al-Ahmed A, Al-Sulaiman FA, Zahir MH, Mohamed SA (2017) Silica fume/capric acid-palmitic acid composite phase change material doped with cnts for thermal energy storage. Sol Energy Mater Sol Cells 179:353–361

Saborío MCG, Lanzalaco S, Fabregat G, Puiggalí J, Estrany F, Alemán C (2018) Flexible electrodes for supercapacitors based on the supramolecular assembly of biohydrogel and conducting polymer. J Phys Chem C 122(2):1078–1090

Shi K, Zhitomirsky I (2013) Polypyrrole nanofiber-carbon nanotube electrodes for supercapacitors with high mass loading obtained using an organic dye as a co-dispersant. J Mater Chem A 1(38):11614–11622

Sundriyal P, Bhattacharya S (2017) Inkjet printed electrodes on A4 paper substrates for low cost, disposable and flexible asymmetric supercapacitors. ACS Appl Mater Interfaces 9(44):38507–38521

Tebyetekerwa M, Wang X, Marriam I, Pan D, Yang S, Zhu M (2017) Green approach to fabricate polyindole composite nanofibers for energy and sensor applications. Mater Lett 209:400–403

Thakur AK, Deshmukh AB, Choudhary RB, Karbhal I, Majumder M, Shelke MV (2017) Facile synthesis and electrochemical evaluation of pani/cnt/mos 2 ternary composite as an electrode material for high performance supercapacitor. Mater Sci Eng B 223:24–34

Tian X, Yang C, Si L, Si G (2017) Flexible self-assembled membrane electrodes based on eco-friendly bamboo fibers for supercapacitors. J Mater Sci: Mater Electron 28(28):1–7

Xu J, Li M, Wu L, Sun Y, Zhu L, Gu S, Liu L, Bai Z, Fang D, Xu W (2014) A flexible polypyrrole-coated fabric counter electrode for dye-sensitized solar cells. J Power Sour 257:230–236

Xu L, Xu J, Yang Y, Mao X, He X, Yang W et al (2018) A flexible fabric electrode with hierarchical carbon-polymer composite for functional supercapacitors. J Mater Sci: Mater Electron 29(3):2322–2330

Yang C, Wang X, Du P, Liu P (2013) Polyaniline/carbon nanotube multi-layered hollow microspheres with sandwich structure and their electrochemical performance. Synth Met 179(5):34–41

Yang N, You TT, Gao YK, Zhang CM, Yin PG (2018) Rapid fabrication of flexible and transparent gold nanorods/poly (methyl methacrylate) membrane substrate for sers nanosensor application. Spectrochim Acta A Mol Biomol Spectrosc 202:376–381

Zhong WB, Liu SM, Chen XH, Wang YX, Yang WT (2006) High-yield synthesis of superhydrophilic polypyrrole nanowire networks. Macromolecules 39:3224–3230